JCAMECH

Vol. 48, No. 2, December 2017, pp 207-216
DOI: 10.22059/jcamech.2017.235183.152

Simulation of the Mode I fracture of concrete beam with cohesive models

Shahriar Shahbazpanahi [1,*], Masoud Paknahad [2]

[1] *Department of Civil Engineering, Sanandaj Branch, Islamic Azad University, Sanandaj, Iran.*

[2] *Faculty of Civil Engineering, Mahallat Institute of Higher Education, Mahallat, Iran.*

Received: 8 June. 2017 , Accepted: 29 Aug. 2017

Abstract

Crack propagation modeling in quasi-brittle materials such as concrete is essential for improving the reliability and load-bearing capacity assessment. Crack propagation explains many failure characteristics of concrete structures using the fracture mechanics approach. This approach could better explain the softening behavior of concrete structures. A great effort has been made in developing numerical models; however, some models involve complex expressions with too many parameters, and the results are in some cases inaccurate. In this investigation, a numerical approach is developed to model the fracture process zone (FPZ). Based on the modified crack closure integral (MCCI) method, a new nonlinear spring is proposed to be placed between the interfacial node pairs to model crack propagation. A new strain energy release rates for Mode I is calculated as a function of opening in the softening part. Two benchmark beams are simulated by the ABAQUS software for the accuracy of cohesive zone model. The model decreases complexity of predicting crack propagation. It is observed that the cohesive zone model is robust, accurate and able to model the crack growth in the concrete beam. The prediction of the crack path is close to the experimental results (up to 90%). The peak loads had approximately 7.7% difference compared with the previous experimental loads. The accuracy of displacement in the present study is 15.9% compared with previously model at the same load intensity.

Keywords: ABAQUS, Fracture, Cohesive, Propagation, Beam.

[*] Corresponding Author. Tel.: +98 918 871 0935; Fax: +98 873 328 8591
Email Address: Sh.shahbazpanahi@iausdj.ac.ir

1. Introduction

Sudden failure occurs in concrete structural members such as beams due to the quasi-brittle behavior of the concrete. In general, sudden failures in concrete structures initiate with crack propagation in the tension zone because of an increase in stress or an occurrence of initial crack. Therefore, these failures should be accurately predicted. Material strength and fracture mechanics theories are two major groups of theories in crack growth analysis. In material strength theory, cracks are detected based on strain, stress, or a combination of stress and strain. The disadvantage of this theory is that eliminating the damaged elements may produce stress singularity. Material strength theory, which existed prior to fracture mechanics, uses a crack propagation criterion with no strain energy effect. It explains the propagation of a crack as an unavoidable method of transferring energy between the strain energy of an elastic body and the fracture energy required to produce a new crack. The fracture mechanics theory is considered to be a more accurate method for predicting crack growth (*1*,*2*), as this method is similar to the physical reality of crack propagation (*3*). Two methods are now available for fracture analysis in concrete structures. These can be broadly categorized into Linear Elastic Fracture Mechanics (LEFM) and nonlinear fracture mechanics. LEFM was first used to study the crack propagation in the warships deployed during World War II (*4*). In this method, a coefficient is applied to the stress in the vicinity of the crack tip (*5*). This coefficient is called the stress intensity factor. Since the stress intensity factor depends on the material properties, the size of the crack, the load, and the geometry of the structure, it presents a relationship between the material and the reaction of the structure. Stress singularity at the crack-tip is a characteristic of LEFM. Later, some studies used LEFM in crack propagation analysis, but Kaplan (*6*) found that the deploying LEFM was not acceptable in solving the crack problems with normal concrete structures (*7*). To solve the aforementioned problem, Hillerborg et al. (8) proposed the first model based on nonlinear fracture mechanics for concrete beam. Their study introduced a region, often termed fracture process zone (FPZ), which has the ability to transfer the normal and shear stress. The FPZ plays a remarkable role in the behavior of the cracks and their propagation under apply loading. Hence a study on the role of the FPZ is indispensable to predict and prevent crack propagation under static monotonic load. Although more techniques of crack propagation have been developed in fracture mechanics, the crack modeling to predict the behavior of concrete structures is still far from satisfactory (*8*). Fracture mechanics have been employed to model crack propagation in concrete with strain-softening behavior (*9*,*10*). To describe the crack propagation criterion in the fracture process at the crack tip, the so-called Griffith energy approach can be used. This approach states that the energy release rate, defined as the amount of energy stored in the FPZ, which is required to form the crack, must be sufficiently larger than the critical fracture energy (*11*). Hence, to study the crack state, the crack propagation criterion can be defined in terms of the energy release rate (*12*,*13*). Hillerborg et al. (*14*) used cohesive stress to simulate the FPZ in cracks. In this model the stress reaches the tensile strength at the tip of the crack and is reduced to zero at the critical opening of the crack (*15*). The area under the stress-opening curve equals to the energy release rate. This model is often referred to as the cohesive zone model (CZM). It is deployed to model the FPZ in normal-size structures (*16*). Either the nodal force release method or an interface element with zero initial thickness is used for this purpose (*17*). CZM was first proposed by Dugdale (*18*) to analyze brittle fracture. Hillerborg et al. (*14*) initially used CZM, also known as the fictitious crack model (FCM), to calculate the approximate softening fracture. In the initial study, they illustrated that crack patterning and growth could be accomplished with CZM, even though a rough finite element was applied. However, by using this method, the mesh sensitivity was reduced. Some studies have been carried out to improve the CZM (*19*). Although CZM has been used with the finite element method, its use has been limited owing to the problems of efficiency and software logistics (*3*). The method proposed by Hillerborg et al. (*14*) has been widely applied because of its practicality, accuracy, and cost effectiveness (*20*). Software, such as the ABAQUS, applies the cohesive zone model (CZM) to demonstrate crack propagation. Two types of interface elements were deployed to develop the CZM. One of the most widely used interface elements was the continuum cohesive zone model (CCZM). The alternative interface element called discrete cohesive zone model (DCZM) was simple to implement (*21*). The DCZM was based on the basic idea that the cohesive zone behaved as a spring. This point of view suggested the use of a spring element between interfacial node pairs instead of a 2-D interface element along the crack path. DCZM was applied in the some investigation in the literature review because this method reduced the computational time and was compatible with the finite element (FE) method (*22*,*23*,*24*). One of the methods for crack propagation modeling (*25*) in the DCZM was the virtual crack closure technique (VCCT). This technique calculates the energy used for closing the crack by multiplying the nodal force and displacement opening. The crack length will increase if the energy release rate is larger than the crack resistance. This method was computationally inexpensive and provided satisfactory results (*26*,*27*).

A great effort has been made in developing numerical models; however some of the developed models have complex expressions involving many parameters, and the

results are somewhat inaccurate (*17*). Thus, the exact model to predict the crack propagation is still under debate. In this investigation, a numerical approach is developed to model the FPZ. Based on the modified crack closure integral (MCCI) method, a new nonlinear spring is proposed to place between the interfacial node pairs in order to model the crack propagation. The new strain energy release rates for Mode I as a function of opening in the softening part can be calculated.

2. Materials and Methods

2.1 Interface element based on DCZM

Modified crack closure integral (MCCI) method is applied to model DCZM for Mode I fracture. Thus, a nonlinear spring is proposed to be placed between the interfacial node pairs (Figure 1). In this figure, the node pairs '1' and '2' have initially the same coordinates. Spring softening is set at the crack tip between the nodes '1' and '2'. Node '3' is a dummy node and it is only used to illustrate the variation in the crack form. The undamaged tangential stiffness matrix, **K**, of the spring related to nodes '1' and '2' are given by:

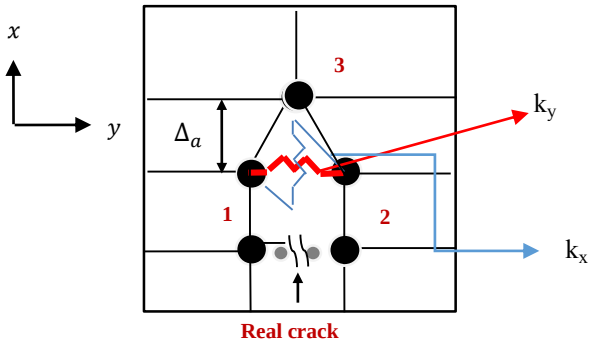

Figure 1. Spring interface element between two nodes

$$\mathbf{K} = \begin{bmatrix} k_x & 0 & -k_x & 0 \\ 0 & k_y & 0 & -k_y \\ -k_x & 0 & k_x & 0 \\ 0 & -k_y & 0 & k_y \end{bmatrix} \quad (1)$$

where k_x and k_y are the stiffness values corresponding to the local coordinates *x* and *y*, respectively. The stiffness matrix is assigned to the AMATRX in the ABAQUS UEL.

During the elastic zone, tangential stiffness matrix can be estimated as:

$$k_x = \frac{GB\Delta_a}{h} \text{ and } k_y = \frac{EB\Delta_a}{h} \quad (2)$$

where B is the thickness of the beam, h is the thickness of the FPZ and Δ_a is the element size. The E and G are Young's modulus and shear modulus, respectively. The elastic zone is defined where $0 < \delta < w_0$. w_0 is the critical opening.

2.2 Discrete Cohesive Zone Model

Figure 2 illustrates the softening stiffness part. A triangular type cohesive law is used in this research. On the softening part of the cohesive law, k_{soft} , stiffness for mode I is determined as:

$$k_{soft} = \frac{\sigma_l}{w} \quad (3)$$

where σ and w are the stress and opening in the softening part, respectively. On other hand, we have:

$$\frac{f_t}{w_c - w_0} = \frac{\sigma_l}{w_c - w} \Rightarrow \sigma_l = \frac{f_t(w_c - w)}{w_c - w_0} \quad (4)$$

where w_c and f_t are the maximum opening and tensile strength of the concrete , respectively. Substituting Eq. (4) into Eq.(3) leads to:

$$k_{soft} = \frac{f_t(w_c - w)}{w(w_c - w_0)} \quad (5)$$

The strain energy release rate for Mode I, G_I, is

$$G_I = \frac{f_t w_c}{2} + \frac{(w - w_0)}{2}(f_t + \sigma) \quad (6)$$

Substituting Eq.(4) into Eq.(6) leads to:

$$G_I = \frac{f_t w_0}{2} + \frac{(w - w_0)}{2}\left(f_t + \frac{f_t(w_c - w)}{w_c - w_0}\right) = \frac{f_t w_c}{2} + \frac{f_t(w_c - w)(w - w_0)}{2(w_c - w_0)}. \quad (7)$$

When $w < w_0$, G_I = 0.0 and k_y is calculated by Eq. (2). When $w_0 < w < w_c$, the softening part of the cohesive law, $k_y = k_{soft}$ and is determined from Eq. (5), G_I is determined from Eq. (7) . When $w > w_c$, k_y is equal to zero, $G_I = G_{Ic}$ and the element is removed. The G_{Ic} is the critical fracture energy of Mode I in the concrete which is the total area under the curve. This formulation is implemented through a user defined subroutine UEL in the ABAQUS.

Shear stress is transferred by fracture zone, k_x, in the tip of crack that it is required to be modeled by interface element. Experimental formulation is applied by Jeang and Hawkins (*28*) to the stiffness values, k_x, corresponding to the local coordinates x.

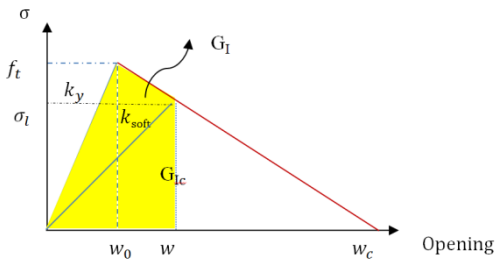

Figure 2. Triangular type cohesive law for the concrete

2. 3 Formulate and Calculate Crack Extension and FPZ Length

Previous modeling of crack propagation regarded crack extension length as the mesh size. Crack extension is related to the ratio of the notch length to the beam depth and the crack opening (*29*) and does not depend on the mesh size, thus, crack extension must be accurately defined in the model. Crack extension is essential in the fracture mechanics and is based on the FPZ length. Crack extension has a linear relationship with the FPZ length until COD reaches 3.6 G_c/f_t, where f_t is the tensile strength of concrete beam. Then, crack extension increases and the FPZ length decreases. Thus, crack extension can be derived as follows (23):

$$\text{If} \quad \Delta u \ll 3.6\frac{G_C}{f_t} : \; L' = l_p(h\text{-}a_0)$$

$$\text{If} \quad \Delta u > 3.6 \; L' = -0.1\, l_p(h\text{-}a_0)+0.91 \quad (8)$$

where L', h and a_0 are the crack extension, the depth of the beam and the length of the initial notch, respectively. Thus, an exact criterion for FPZ length is necessary to estimate the crack extension. The present study used the experimental results of Xu et al. (*23*) to evaluate FPZ length. Figure 3 (a) shows an effective crack, in which l_p, $a_{\sigma=0}$, and a are the FPZ length, the stress-free region length, and effective crack length, respectively.

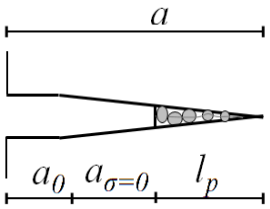

(a) Effective Crack

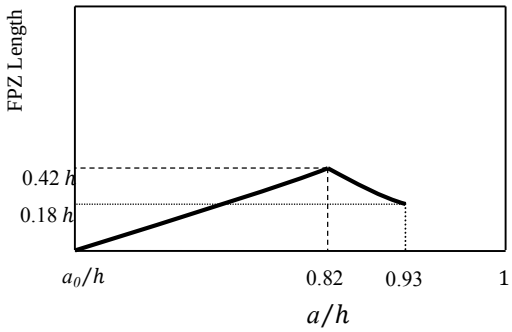

(b) Variation of FPZ Length

Figure 3. Crack extension and FPZ length for concrete beam obtained by the experimental results of Xu et al. (23)

Figure 3 (b) illustrates the linear relationship between the FPZ length and the effective crack length (Xu et al., 2011). The FPZ length initially increases up to the maximum value of 0.42 h at a= 0.82 h and then decreases until it reaches the value of 0.18 h at a =0.93 h. The advantage of the present model is that the size effect on the FPZ length is considered based on the aforementioned approach.

Moreover, when the FPZ length is fully extended and reaches the maximum rate, the stress-free length occurs in front of the notch or the macro-crack behind the FPZ (Wu et al., 2011), this finding was not considered by previous researches. An accurate explanation of propagation and crack formation must be considered in the model, such as a stress-free region length formulated in finite element methods as follows:

$$a_{\sigma=0}=N \times \Delta_a \quad (9$$

where $a_{\sigma=0}$ and N are the stress-free region length and the number of elements that have failed behind FPZ, respectively. When FPZ is fully propagated, the N element is set to zero behind the crack and the crack grows along the respective element. The direction is considered at each step. For the first time, this stress-free region is considered and formulated using the FE method to predict the crack propagation accurately.

Another issue to model the crack is its direction. The initial direction of the propagation is usually unknown. Thus, many researchers proposed to use the approximate re-meshing algorithms. In such algorithms, a significant number of nodes are created for re-meshing; resulting in creating large stiffness matrices, splitting some of the elements, and increasing the computational complexity and time. An alternative method is the inter-element boundaries technique which directs the crack path. In this investigation, the crack follows existing the inter-element boundaries and no re-meshing algorithm is needed. The orientation angle (θ) of element is (Figure 4):

$$\cos\theta = \frac{y_3\text{-}y_1}{\sqrt{(x_3\text{-}x_1)^2 + (y_3\text{-}y_1)^2}} \qquad (10)$$

where x_1 and y_1 are the coordinates of the components node '1' and x_3 and y_3 are the coordinates of the components node '3'. In this investigation, the direction of the crack is implemented by a method in which the crack follows the existing inter-element borders. This method has a simple algorithm and there is no need for re-meshing. Crack propagation follows one of the inter-elements (AB) or (AC) paths where it is assumed that the crack will not stop and intersect the main element (Figure 4). There are two possible cases for the crack path; if the orientation angle (θ), is less than 45°, the growth path is AB, otherwise AC.

The stiffness matrix, the nodal forces and the displacements can be transformed in the local (x, y) system to the global system (X,Y) by using the transformation matrix.

3. Results and discussion

This section provides an additional check for the accuracy of the DCZM compared with the previous experimental results and other numerical results on concrete beams. Two benchmark beams are simulated (16) by the ABAQUS software, which have been reported in the literature.

Figure 5 shows the tested plain, the four-point single-edge notched shear beam by Arrea and Ingraffea (*30*). This beam was considered a benchmark for crack propagation analysis. The material properties of the concrete were 24,800 MPa for the Young's modulus, 0.18 for the Poisson's ratio, and 4 MPa for the tensile strength. The thickness of the beam was 152 mm, and the length of the initial notch was 82 mm. The parameter values of the fracture were G_c=150 N/m, w_c = 0.135 mm, and w_0 = 0.0001 mm. The dimensions of the mesh elements should be fine in the area of the possible cracking to obtain the accurate results.

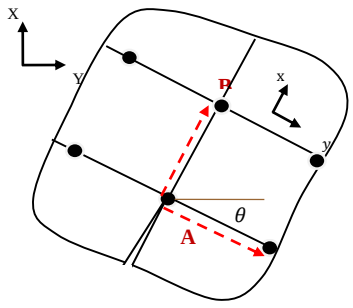

Figure 4. Two Possible cases for the direction of propagation

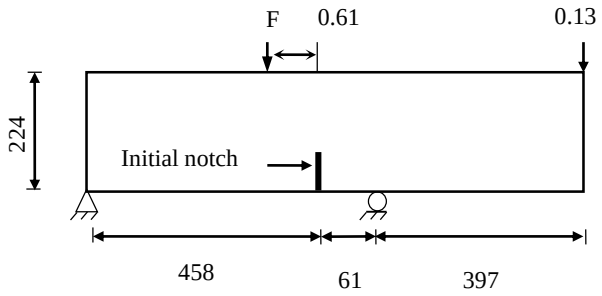

Figure 5 Four-point single-edge notched shear beam

Figure 6 indicates the load versus the crack mouth sliding displacement curve by the ABAQUS software result, which were compared with the experimental results (*30*), a model of Xie and Gerstle (*31*). The beam was modeled by the ABAQUS software with 7,899 C3DBR elements (the average size was 1.5 mm × 1.5 mm). The figure shows that the peak loads were close to each other. The present numerical results were acceptable compared with that of the experimental envelope. The accuracy of the peak loads compared with modeled proposed by Xie and Gerstle (30) was 29.5%. In the softening zone after 60 kN, the present model showed better agreement in terms of the ductility observed in the experimental results than the proposed model by Xie and Gerstle (30). This may be due to the stress-free zone, the crack extension and the FPZ length in the tip of the notch was not considered in previous models such as modeled by Xie and Gerstle (30). In the elastic part, the cure rests on the mid-point of the previous experimental results (*30*). The difference between the proposed model and the experimental result was inevitable because the behavior of concrete was assumed to be linear elastic in the fracture mechanics. However, in reality, concrete is nonlinear plastic.

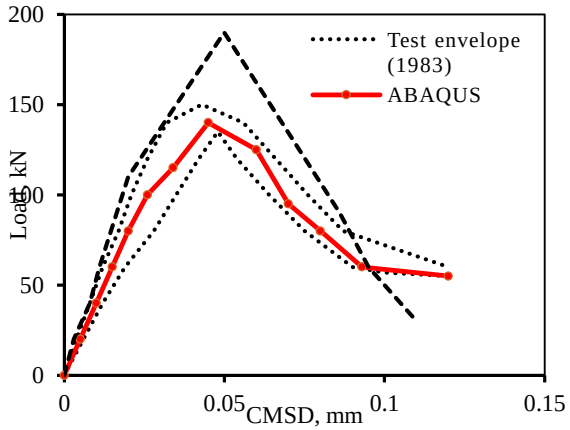

Figure 6. Load-CMSD curves for shear beam

The peak loads had approximately 7.7% difference compared with the experimental load. After the peak load, the curve in the softening zone (up to 55 kN), which turned

slightly brittle, were closer to the experimental result than the numerical model (*31*). In the softening zone after 55 kN, the present model showed better agreement in terms of the ductility observed in the experimental results than the previous studies. This finding is attributed to the fact that the stress-free zone at the tip of the notch was not considered in the modeling.

As shown in Figure 7, the results from the conventional VCCT and CCZM is performed without considering the variations of the FPZ length and the crack extension. It can be seen that the results do not agree with the experimental data and in the elastic zone, the stiffness of the beam in conventional VCCT and CCZM are more than in the experimental data. Also, the peak loads from the conventional VCCT and CCZM are larger than those of the experimental and proposed DCZM.

As shown in Figure 8, Mesh (a) had 864 elements [the element average size is 1.7 mm × 1.3 mm, with finer mesh (15 mm × 1.0 mm) at the initial notch area] and 324 interface elements. Mesh (b) had 1,026 elements [element average size is 1.5 mm × 1.0 mm, with finer mesh (1.4 mm ×0. 9 mm) at the initial notch area] and 508 interface elements. Mesh (c) had 1,862 elements [the element average size is 1.2 mm × 0.8 mm, with finer mesh (1.0 mm × 0.5 mm) at the initial notch area] and 875 interface elements. The approximate matching of the three curves demonstrates the independence of the model from the mesh size and shows that the model exhibited fast convergence. Although, the mesh size was changed in the model, no significant change in the peak load was observed.

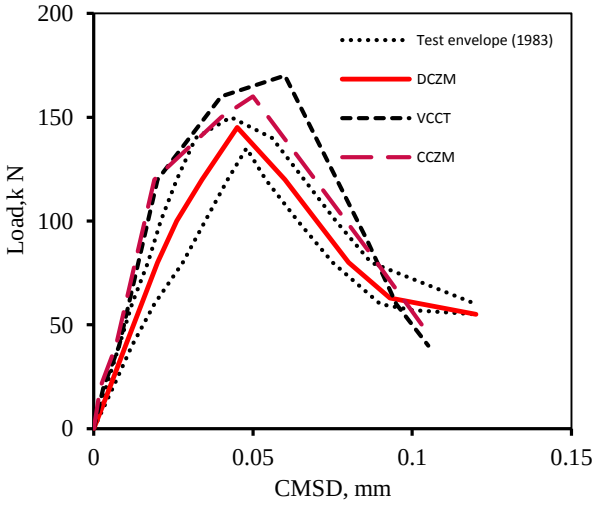

Figure 7.Comparisons of Load-CMOD curves for proposed DCZM, conventional VCCT and CCZM

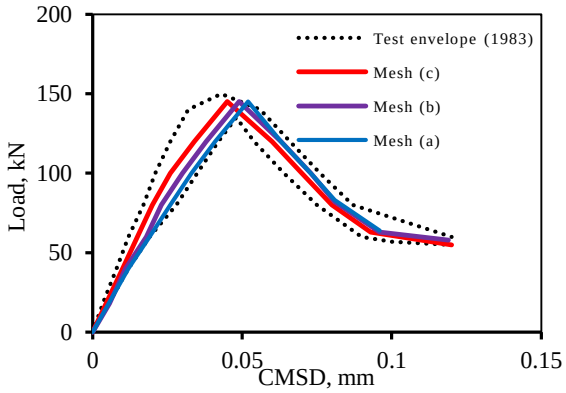

Figure 8. Comparison between three meshes with the experimental results (29)

Figure 9 (a) shows the predicted crack path, which is compared with the results from the experimental test obtained [Figure 9 (b)]. The prediction of the crack path was close to the experimental results (up to 90%). The FPZ propagation elements are shown in red lines, while the stress-free elements are displayed in black. It should be noted that the crack path is smooth, although in this study the crack path is illustrated by unconventional lines. The tensile damage is defined from 0 to 0.1 in the ABAQUS software. The result showed that the maximum value of the damage parameter is 0.407 > 0.1. Therefore, the tensile damage occurred near the notch and along red lines as shown in Figure 9 (a).

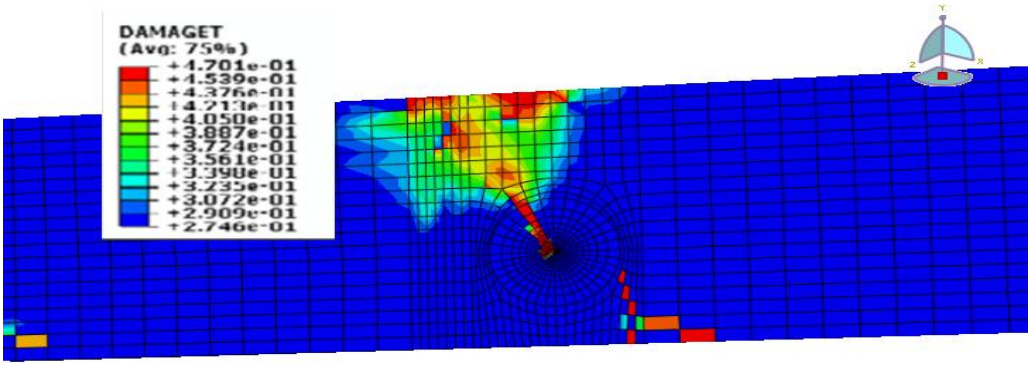

(a) Result of the ABAQUS software

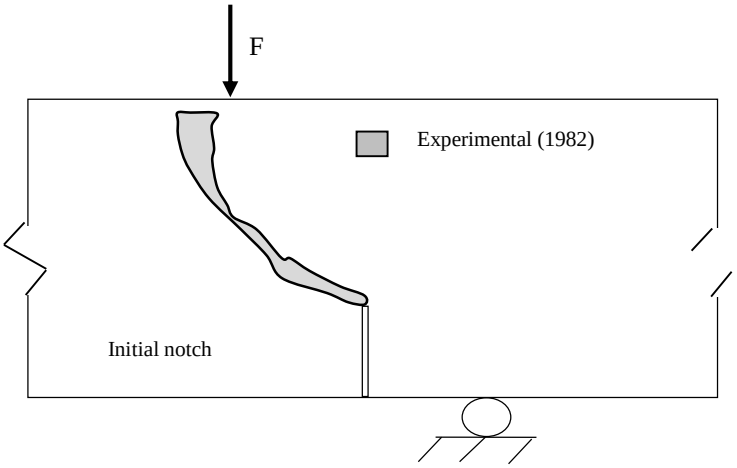

(b) Test results (31)

Figure 9. Crack paths in the shear beam

The second example was a reinforced concrete beam with simple supports (Figure 10), which was tested by Bresler and Scordelis (*32*). This beam test, which was performed by Bresler and Scordelis (*32*), has been widely used for validating nonlinear FE models to simulate the behavior of RC structures (*33*). The geometry of the RC beam was 4,572 mm long and 305.8 mm thick. The material properties of the plastic were 24,000 MPa elastic modulus and 0.18 Poisson's ratio, whereas that of the steel were 200 GPa the elastic modulus, 0.3 the Poisson's ratio, 3,290 mm2 cross-sectional area, and 552 MPa yield strength. The tensile strength of the concrete was 2.8 MPa and COD was critical at 0.152 mm. The two-node truss element was used to model the steel bar with perfect plastic behavior. The beam was not reinforced with stirrups. The analysis considered plane stress, and half of the beam was simulated for modeling in the symmetrical condition (Figure 10).

The bond between the longitudinal bars and the concrete was assumed perfect. The load versus the deflection curve at the mid-span of the beam is compared with the experimental result (*32*), and the analysis results of Arrea and Ingraffea (*30*), as shown in Figure 11. The beam was modeled by the ABAQUS software with 4,814 C3DBR S4R elements (the average size was 1.7 mm × 1.7 mm × 1.7 mm).

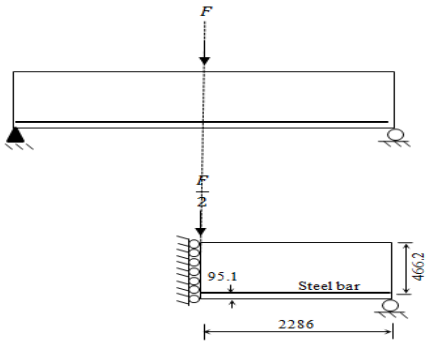

Figure 10. Half of the RC beam (Unit: mm)

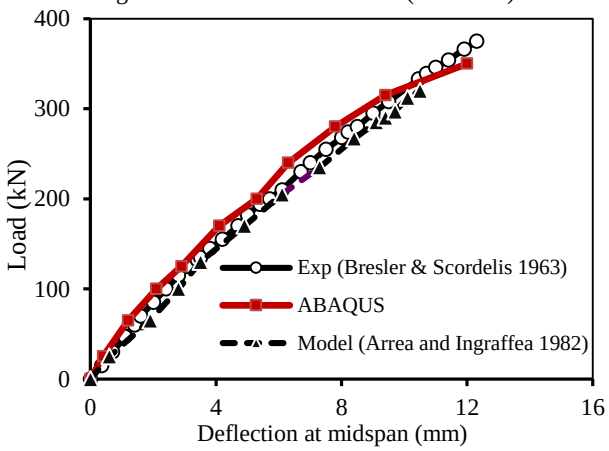

Figure 11. Comparison of load-deflection at the mid-span

The stiffness in the present study was slightly higher than that in the experimental observation (approximately 10%). This error may be acceptable because the crushing, nonlinear behavior of the concrete and the plastic deformation were neglected in the fracture mechanics. The accuracy of the displacement in the present study compared with modeled by Arrea and Ingraffea (*30*) is 15.9% at the same load of 300 kN.

Figure 12(a) shows the crack paths in the present study. Figure 12(b) shows the crack patterns at a load of 285 kN in the experimental study (*32*). Flexural cracks occur under the initial load. The effective crack length was 10.2 mm at 54 kN load in the vicinity of the mid-span and 262.7 mm at 100 kN load. Shear crack started at approximately 170 kN load at the support and expanded upward as the load increased.

The experimental model shows 13 cracks, including the flexural and shear cracks. These cracks incline toward the load, except for the first crack. A total of 14 cracks were predicted in the present model, in which the 2 cracks near the mid-span did not detour. Given that the single-active-crack mode strategy was used to simulate multiple cracks as proposed by Shi et al. (*7*), the results showed that the predicted crack patterns were close. Therefore, the model presented in this study showed acceptable similarity to the previous experimental results.

4. Conclusion

In this study fracture mechanics is implemented to model cracks propagation with strain softening behavior in concrete beam. The cohesive zone model is used by the finite element method to model the Mode I fracture of the concrete beam. A nonlinear spring is proposed to be placed between interfacial node pairs to model the crack propagation. As a function of opening in the softening part, strain energy release rates for Mode I can be calculated at the same time. Two benchmark beams are simulated by the ABAQUS software for the accuracy of the cohesive zone model. It is observed that the cohesive zone model is robust, accurate and it is able to model the crack growth in the concrete beam. The prediction of the crack path was close to the experimental result (up to 90%). The peak loads had approximately 7.7% difference compared with the previous experimental load. The difference between the displacements in the present study compared with the previous model at the same load is 15.9%. The simulation results are close to the available experimental results. This model improves the result of the analysis of discrete crack propagation.

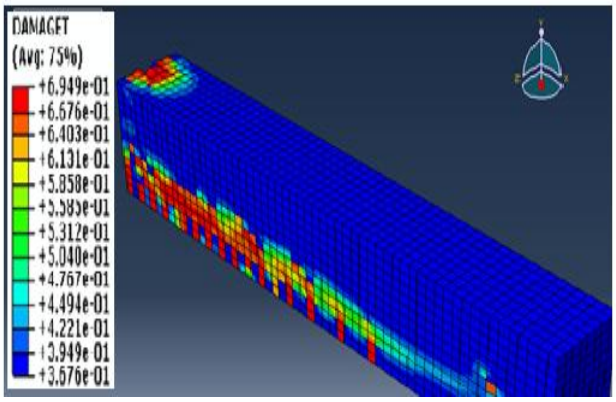

(a) Crack predicted by the ABAQUS software

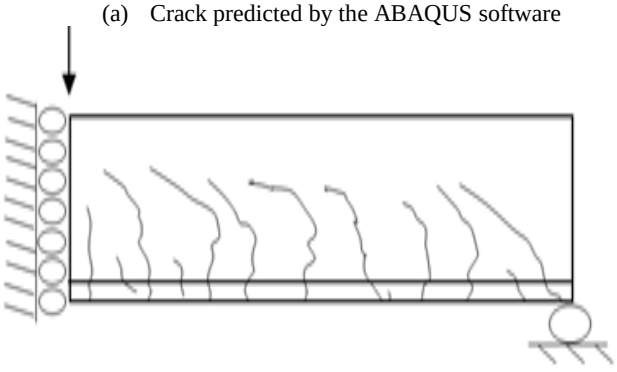

(b) Crack predicted by test result (33)

Figure 12. Crack predicted at 285 kN load

5. References

[1] Shahbazpanahi, S., Kamgar, A., 2015, A novel numerical model of debonding of FRP-plated concrete beam. Journal of the Chinese Institute of Engineers, 8, 24-32.

[2] Shahbazpanahi, S.; Hejazi, F.; Paknahad, M.; Rahimipour, A.; Nassimi, M. R., 2018,Modeling crack propagation in RC beam–column joints. *Tehnički Vjesnik - Tehnical Gazette*, In Press.

[3] Shi, Z. Crack analysis in stuctural concrete, theory and aplication; Butterworth-Heinemann: Burlington, USA, 2009.

[4] Esfahani, M. R., 2007, Fracture mechanics of concrete, Tehran Polytechnic press: Tehran Iran.

[5] Shahbazpanahi, S.,2017, Mechanical analysis of a shear-cracked RC beam. Acta Scientiarum. Technology **,** 39 (3), 285-290.

[6] Kaplan, M. E., 1961, Crack propagation and the fracture concrete. ACI Journal, 58 (5), 591- 610.

[7] Shi, Z., Ohtsu, M., Suzuki, M., Hibino, Y., 2001, Numerical analysis of multiple cracks in concrete using the discrete approach. J. Struct. Eng., 127 (9), 1085-1091.

[8] Shahbazpanahi, S., Ali, A. A. A., Aznieta, F. N., Kamgar, A., Farzadnia, N., 2013, A simple and practical model for FRP-reinforced cracked beam. European Journal of Environmental and Civil Engineering, 18(3), 293-306.

[9] Kiranea, K., Bazant, Z., 2015, Size effect in Paris law for quasibrittle materials analyzed by themicroplane constitutive model M7. Mechanics Research Communications, 60-64.

[10] Dong, W., Yang, D., Kastiukas, G., Zhang, B., 2016, Experimental and numerical investigations on fracture process zone of rock-concrete interface. Fatigue and Fracture of Engineering Materials and Structures, 40(5), 820-835.

[11] Ouzaa , K., Benmansour, M. B., 2014, Cracks in continuously reinforced concrete pavement. Arabian Journal for Science and Engineering, 39, 8593-8608.

[12] Shahbazpanahi, S., Ali, A. A. A., Aznieta, F. N., Kamkar, A., Farzadnia, N., 2013, Modelling of the fracture process zone to improve the crack propagation criterion in concrete. Journal of the South African Institution of Civil Engineering, 55 (3), 2- 9.

[13] Biscaia, H. C., Chastre, C., Silva, M. A. G., 2014, Linear and nonlinear analysis of bond-slip models for interfaces between FRP composites and concrete. Composites: Part B, 45, 1554-1568.

[14] Hillerborg, A., Modeer, M., Petersson, P. E., 1976, Analysis of crack formation and crack growth in concrete by means of mechanics and finite element. Cement and Concrete Research, 6, 773-782.

[15] Dong, W., Wu, Z., Zhou, X., Dong , L., Kastiukas, G. FPZ evolution of mixed mode fracture in concrete: Experimental and numerical. Engineering Failure Analysis 2017, 75.

[16] Shahbazpanahi, S., Ali, a. a. a., Aznieta, F., Kamgar, A., Farzadnia, N., 2012, A simple method to model crack propagation in concrete. Constructii Journa, 13 (1), 41-50.

[17] Yang, Z. J., Liu, G., 2008, Towards fully automatic modelling of the fracture process in quasi-brittle and ductile materials: a unified crack growth criterion. Journal of Zhejiang university science, 9 (7), 1862-1775.

[18] Dugdale, D. S., 1960, Yielding of steel sheets containing slits. J Mech Phys Solid, 8 (2), 100-104.

[19] Shahbazpanahi, S., Abang, A. A., Aznieta, F., Kamgar, A., Farzadnai, N. A, 2014, Theoretical method for fracture resistance of shear strengthened RC beams with FRP, 39(5), 3591-3597.

[20] Palmieri, V., Lorenzis, L. D., 2014, Multiscale modeling of concrete and of the FRP-concrete interface. Engineering Fracture Mechanics, 131, 150-175.

[21] Said, A. M., Nehdi, M. L., 2004,Use of FRP for RC frames in seismic zones:Part I. Evaluation of FRP beam-column joint rehabilitation techniques. Applied Composite Materials, 11, 205-226.

[22] Xie, D., Waas, A. M., 2006, Discrete cohesive zone model for mixed-mode fracture using finite element analysis. Engineering Fracture Mechanics, 73 (13), 1783-1796.

[23] Xu, F., Wu, Z., Zheng, J., Zhao, Y., Liu, K., 2011, Crack extension resistance curve of concrete considering variation of FPZ length. J. Mate. Civ. Eng., ASCE, 23 (5), 703-710.

[24] Simon, K. M., Kishen,. A, 2017, Multiscale approach for modeling fatigue crack growth in concrete. International Journal of Fatigue, 98, 1-13.

[25] Shokrieh, M. M., Rajabpour-Shirazi, H., Heidari-Rarani, M., Haghpanahi, M., 2012, Simulation of mode I delamination propagation in multidirectional composites with R-curve effects using VCCT method. Computational Materials Science, 65, 66-73.

[26] Xie, D., Salvi, A. G., Sun, C., Waas, A. M., Caliskan, A. I., 2006, Discrete Cohesive Zone Model to Simulate Static Fracture in 2D Triaxially Braided Carbon Fiber Composites. Journal of Composite Materials 2006, 40(22), 2025- 2046.

[27] Xie, D., Biggers, S. B. J., 2006, Progressive crack growth analysis using interface element based on the virtual crack

closure technique. Finite Elements in Analysis and Design, 42 (11), 977 - 984.

[28] Jeang, F. L. Hawkins, N. M., 1985, Non-linear analysis of concrete fracture; Report No. SM 85-2; University of Washington: USA.

[29] Wu, Z., Rong, H., Zheng, J., Xu, F., 2011, An experimental investigation on the FPZ properties in concrete using digital image correlation technique. Engineering Fracture Mechanics, 78 (17), 2978-2990.

[30] Arrea, M., Ingraffea, A. R., 1982, Mixed-mode crack propagation in mortar and concrete, Report No. 81-13, Department of Structural Engineering: Cornell University.

[31] Xie, M., Gerstle, W. H., 1995, Energy-based cohesive crack propagation modeling. Journal of Engineering Mechanics, ASCE, 121 (12), 1349-1458.

[32] Bresler, B., Scordelis, A. C., 1963, Shear strength of reinforced concrete beams. American Concrete Institute, ACI, 60 (40), 51-72.

[33] Yang, Z. J., Chen, j., 2005, Finite element modelling of multiple cohesive discrete crack propagation in reinforced concrete beams. Engineering Fracture Mechanics, 72 (14), 2280-2297.